
RANK-ADAPTIVE SPECTRAL PRUNING OF CONVOLUTIONAL LAYERS DURING TRAINING

Emanuele Zangrando*
Gran Sasso Science Institute
67100 L'Aquila (Italy)
emanuele.zangrando@gssi.it

Steffen Schotthöfer*
Karlsruhe Institute of Technology
76131 Karlsruhe (Germany)
steffen.schotthoefner@kit.edu

Gianluca Ceruti
EPF Lausanne
1015 Lausanne (Switzerland)
gianluca.ceruti@epfl.ch

Jonas Kusch
University of Innsbruck
6020 Innsbruck (Austria)
jonas.kusch1@gmail.com

Francesco Tudisco
Gran Sasso Science Institute
67100 L'Aquila (Italy)
francesco.tudisco@gssi.it

ABSTRACT

The computing cost and memory demand of deep learning pipelines have grown fast in recent years and thus a variety of pruning techniques have been developed to reduce model parameters. The majority of these techniques focus on reducing inference costs by pruning the network after a pass of full training. A smaller number of methods address the reduction of training costs, mostly based on compressing the network via low-rank layer factorizations. Despite their efficiency for linear layers, these methods fail to effectively handle convolutional filters. In this work, we propose a low-parametric training method that factorizes the convolutions into tensor Tucker format and adaptively prunes the Tucker ranks of the convolutional kernel during training. Leveraging fundamental results from geometric integration theory of differential equations on tensor manifolds, we obtain a robust training algorithm that provably approximates the full baseline performance and guarantees loss descent. A variety of experiments against the full model and alternative low-rank baselines are implemented, showing that the proposed method drastically reduces the training costs, while achieving high performance, comparable to or better than the full baseline, and consistently outperforms competing low-rank approaches.

1 Introduction

A main limitation of state-of-the-art neural networks is their memory consumption and computational costs for inference and, especially, training. Leveraging well-known parameter redundancies [10, 4, 14], a large body of research work has been dedicated to removing redundant information from weights to reduce the memory and computational footprints. Such efforts include weight sparsification [17, 38, 20] and quantization [54, 12]. Despite their considerably reduced resource requirements for inference, these methods cannot achieve memory reduction during training. As pointed out in [14], training sparse neural networks from the start is challenging, and re-training accurate sparse architectures obtained through pruning with random initialization is commonly impossible. At the same time, as model and data size grow, the training phase of modern architectures can require several days on several hundreds of GPUs [3]. Thus, being able to reduce the resource demand of the training phase while maintaining model performance is of critical importance.

The gap between the existing methods to construct highly efficient networks for inference and the inability to efficiently determine such networks during training has been addressed by low-rank training methods

*These authors contributed equally to this work.

[51, 22, 42]. These methods aim to find high-performing low-rank subnetworks *during* training. I.e., instead of training full-weight matrices and pruning in a subsequent step, low-rank factorizations of weight matrices exploit the Riemannian structure of the manifold of low-rank matrices to train the networks directly within the manifold. In this way, no full-rank matrix needs to be constructed as the algorithms solely work with low-rank weight matrices.

Low-rank training of feed-forward fully-connected neural networks can reduce training costs by more than 90%, while maintaining approximately the same accuracy of the full model [42, 51, 22]. However, these methods struggle to efficiently handle convolutional layers. In fact, efficiently compressing convolutional layers is a major challenge for most pruning and parameter reduction techniques [9, 37]. Another main challenge of low-rank training techniques is the dependence of the training convergence on the conditioning of the weight matrices [42] due to the high curvature of the low-rank manifold [25], which may result in slow convergence rates and poor performance [51, 22, 42, 29].

1.1 Contribution

In this work, we introduce a novel low-rank training algorithm that directly aims at bridging the above gaps by efficiently handling convolutional layers leveraging recent advances on dynamical low-rank approximation [5, 6]. Available low-rank training methods [51, 22, 42, 21, 55] often treat convolutional layers by performing a matricization of the convolutional tensors. However, this procedure is computationally costly and reduces the flexibility of the low-rank representation, failing to properly capture relevant low-rank representations of the convolutional layers and thus resulting in poor compression performance. In this work, we propose a training algorithm that directly trains on modes of Tucker tensors. The proposed method offers three significant enhancements over previous approaches. First, the algorithm is *computationally efficient* for convolutional layers as it reduces computationally costly matricizations of tensors. Second, the Tucker representation *improves the approximation quality* of the low-rank representation while adaptively learning the approximating ranks of *every* mode individually. Third, the convergence is not slowed down by the curvature of the low-rank manifold, i.e., the method shares the desirable *robustness properties* of [42]. As a result, the proposed method yields in certain cases (e.g. VGG16 on CIFAR10) **more than 95% training compression**, while achieving **comparable or better accuracy** performance than the full baseline model. On top of extensive numerical evidence, we provide two important theoretical results showing that (a) the method’s convergence does not suffer the high-curvature of the Tucker low-rank manifold and thus potential ill-conditioning of the layers, and (b) the computed low-Tucker-rank network well-approximates the ideal full model, providing a form of constructive proof of the low-rank lottery ticket hypothesis.

The paper is structured as follows: After the introduction, we discuss the representation of convolutional filters as low-rank Tucker tensors in Section 2. In Section 3 we present the novel method which trains convolutional layers using the Tucker tensor format. Lastly, we underline the effectiveness of the method in Section 4 by a series of computational experiments.

1.2 Related work

Related work on neural network compression methods differs structurally by the mathematical object of consideration, i.e. matrix- or tensor-valued parameter structures, as well as the manifestation of parameter reduction. Related works as pruning of weight matrices [19, 40, 47] and tensors [38, 52] enable parameter reduction by enforcing sparsity, i.e. zero-valued entries, of the weight structures, whereas low-rank compression imposes parameter reduction by factorization of weight matrices [21, 31, 51] and tensors [29, 45, 1, 41, 28, 24, 28, 46]. Besides approaches that transform tensor layers into compressed matrices [42, 21, 31, 51], different tensor decompositions have been employed to compress convolutional layers. Such approaches include CP decomposition [29, 45, 1, 41], Tucker [28, 24], tensor trains [28, 46] or a combination of these [15]. Other methods consider only the floating point representation of the weight structures, e.g. [49, 16, 18, 11, 50], or a combination of the above [32].

From the algorithmic point of view, related work can be categorized into methods to compress fully-trained networks entirely in a postprocessing step after a full-scale training is performed [39, 36, 29, 24, 15, 1], iterative methods where the network is pre-trained and subsequently compressed and fine-tuned [19, 21, 51], and methods that directly compress networks dynamically during training [42, 40]. The latter method

type provides the most potential to reduce the overall computational footprint since no full-scale training is needed.

Only a few of these methods propose strategies for dynamical compression during training or fine-tuning, e.g. by finding the rank via alternating, constraint optimization in discrete [30] and discrete-continuous fashion [21]. However, both these approaches require knowledge of the full weight matrix (and often of its singular value decomposition) during training and overall are more computationally demanding than standard training. In [42], rank-adaptive evolution of the gradient flow on a low-rank manifold was proposed to train and compress networks without the usage of the full weight representation, however only for matrix-valued layers.

The development of a dynamical low-rank training for tensor-valued layers poses non-trivial challenges as the factorization format, the preservation of descent directions, and the accuracy estimates of the resulting models. Numerical instabilities arising from the CP decomposition during training had been mentioned in [29], and in [41] the authors proposed a solution addressing this issue. To the best of our knowledge, in none of the previously cited methods for tensor decomposition of networks, the problem of the intrinsic stiffness of optimizing directly on low-rank manifolds has been addressed.

2 Low-rank Tucker representation of convolutional layers

Neural networks' convolutional filters are the backbone of many groundbreaking machine learning architectures. These layers are defined by a convolutional kernel which consists of a four-mode tensor $W \in \mathbb{R}^{n_1 \times n_2 \times n_3 \times n_4}$, where n_1 is the number of output channels, n_2 is the number of input channels and (n_3, n_4) are the spatial dimensions of the filter. A kernel represents n_1 convolutional filters of shape $n_2 \times n_3 \times n_4$, which are applied to the input embedding tensor $Z \in \mathbb{R}^{N \times n_2 \times N_1 \times N_2}$, where N is the batch size and (N_1, N_2) are the spatial dimensions of the embedding's channel. The convolution operation $W * Z$ is then defined as

$$(W * Z)(i_1, i_2, i_3, i_4) = \sum_{j_2=1}^{n_2} \sum_{j_3=1}^{n_3} \sum_{j_4=1}^{n_4} W(i_2, j_2, j_3, j_4) Z(i_1, j_2, i_3 - j_3, i_4 - j_4). \quad (1)$$

Convolutions are linear operations on tensor blocks. To enable the use of matrix techniques, a standard approach to handle convolutional layers is via a matricization step, in which the tensor W is reshaped into a matrix $\widetilde{W} \in \mathbb{R}^{n_1 \times n_2 n_3 n_4}$ and the input embedding Z into a third-order tensor $\widetilde{Z} \in \mathbb{R}^{N \times n_2 n_3 n_4 \times L}$ obtained by stacking L blocks of the vectorized version of Z following the sliding patterns of the kernel. With this reshaping, the convolution operation (1) coincides with a batch matrix-matrix product

$$(W * Z)(i_1, i_2, i_3, i_4) = \sum_{j_2 j_3 j_4=1}^{n_2 n_3 n_4} \widetilde{W}(i_2, j_2 j_3 j_4) \widetilde{Z}(i_1, j_2 j_3 j_4, i_3 i_4), \quad (2)$$

where indices that are juxtaposed denote linear indices after the reshaping. The above matrix representation allows, in particular, to represent the convolution in terms of a low-rank matrix factorization, an approach that is widely adopted by the recent literature [42, 21, 55, 51, 22]. Even though it is possible, this matricization operation is too restrictive as a representation as it destroys the structure of the convolutional kernel and does not allow capturing compressible modes in the higher-order sense. For this reason, low-rank pruning techniques have consistently failed to achieve significant memory footprint reduction of convolutional layers by using a low-rank approximation of \widetilde{W} in the neural network architecture, see Figure 1 and Table 1. On the other hand, it is well-known that low-rank decompositions based on higher-order tensor ranks can provide much better representations of compressed convolutional layers [46, 45, 15, 31, 28]. Among the various tensor-rank formats, the Tucker rank is arguably the best known in data applications as it is directly based on the so-called Higher-Order SVD (HOSVD) [13].

The Tucker representation maintains the convolutional structure and represents the rank of each mode in the filter individually. In this paper, we use the Tucker decomposition to represent low-rank convolutional layers in tensor format and thus design an algorithm that trains using only the low-rank factors, while simultaneously adjusting the Tucker ranks. The higher-order rank format allows capturing high-performing low-rank substructure along each of the four modes of the kernel individually, which would be blended

together, instead, after the matricization step. Below we review the Tucker representation of a convolutional layer, and we will present the new training algorithm next.

2.1 Tucker representation of a convolutional filter

For a tensor W we write $\text{Mat}_i(W)$ to denote the matrix obtained by unfolding W along its i -th mode. The tuple $\rho = (r_1, r_2, \dots, r_d)$ is called Tucker rank of W if $r_i = \text{rank}(\text{Mat}_i(W))$. Every fourth-order tensor W with Tucker rank $\rho = (r_1, \dots, r_4)$ can be written in Tucker form (or Tucker decomposition) $W = C \times_1 U_1 \times_2 U_2 \times_3 U_3 \times_4 U_4 = C \times_{i=1}^4 U_i$, entrywise defined as

$$W(i_1, i_2, i_3, i_4) = \sum_{\alpha_1=1}^{r_1} \cdots \sum_{\alpha_4=1}^{r_4} C(\alpha_1, \alpha_2, \alpha_3, \alpha_4) U_1(i_1, \alpha_1) U_2(i_2, \alpha_2) U_3(i_3, \alpha_3) U_4(i_4, \alpha_4), \quad (3)$$

where $C \in \mathbb{R}^{r_1 \times \dots \times r_4}$ is a *core tensor* of full Tucker rank $\rho = (r_1, \dots, r_4)$ and the $U_i \in \mathbb{R}^{n_i \times r_i}$ are matrices with orthonormal columns. Note that in terms of the i -th unfolding, (3) reads $\text{Mat}_i(W) = U_i S_i V_i^\top$ with $S_i = \text{Mat}_i(C)$ and $V_i = \otimes_{j \neq i} U_j$, i.e. the usual matrix decomposition.

Using this decomposition, the convolution with kernel W can be written completely in terms of the factors U_i and the core C . In fact, if we let

$$A(\alpha_2, \alpha_3, \alpha_4, i_1, i_3, i_4) = \sum_{j_2, j_3, j_4} U_2(j_2, \alpha_2) U_3(j_3, \alpha_3) U_4(j_4, \alpha_4) Z(i_1, j_2, i_3 - j_3, i_4 - j_4)$$

where $A = (U_2 \otimes U_3 \otimes U_4) * Z$ is the convolution with the factorized kernel $(U_2 \otimes U_3 \otimes U_4)$, then

$$(W * Z)(i_1, i_2, i_3, i_4) = \sum_{\alpha_1, \dots, \alpha_4} C(\alpha_1, \alpha_2, \alpha_3, \alpha_4) A(\alpha_2, \alpha_3, \alpha_4, i_1, i_3, i_4) U_1(i_2, \alpha_1),$$

which we can compactly write as

$$W * Z = C \times_{2,3,4} [(U_2 \otimes U_3 \otimes U_4) * Z] \times_1 U_1.$$

From this representation, we immediately see that if W is represented in Tucker format, then the cost of storing W and of performing the convolution operation $W * Z$ is $O(r_1 r_2 r_3 r_4 + n_1 r_1 + n_2 r_2 + n_3 r_3 + n_4 r_4)$, as opposed to the $O(n_1 n_2 n_3 n_4)$ cost required by the standard full representation. Clearly, when $n_i \gg r_i$, for example $n_i > 1.5 r_i$, the latter is much larger than the former. As an example, for Alexnet trained on Cifar10 the third convolutional layer has Tucker ranks $[r_1, \dots, r_4] = [115, 57, 3, 3]$ (with $[n_1, \dots, n_4] = [384, 192, 3, 3]$). Thus, we have that the memory complexity of the compressed Tucker format is $5.19 \times 1.14 \times 10^5$ versus 6.63×10^5 elements to be stored, i.e., compression of 82.8% on that layer (Appendix A in the supplementary material and Section 4.2).

3 Dynamical low-rank training of convolutions in Tucker format

For $\rho = (r_1, r_2, r_3, r_4)$, the set $\mathcal{M}_\rho = \{W : \text{rank}(\text{Mat}_i(W)) = r_i, i = 1, \dots, 4\}$ is a manifold with the following tangent space at any point $W = C \times_{i=1}^4 U_i \in \mathcal{M}_\rho$ [26]

$$T_W \mathcal{M}_\rho = \left\{ \delta C \times_{i=1}^4 U_i + \sum_{j=1}^4 C \times_j \delta U_j \times_{k \neq j} U_k : \delta C \in \mathbb{R}^{r_1 \times \dots \times r_4}, \delta U_j \in T_{U_j} \mathcal{S}_j \right\} \quad (4)$$

where \mathcal{S}_j is the Stiefel manifold of real $n_i \times r_i$ matrices with orthonormal columns. To design a strategy that computes convolutional filters within \mathcal{M}_ρ using only the low-rank Tucker factors C and $\{U_i\}_i$, we formulate the training problem as a continuous-time gradient flow projected onto the tangent space (4). As shown in Section 3.2, the continuous formulation will allow us to derive a modified backpropagation pass which uses only the individual small factors $C, \{U_i\}_i$ and that does not suffer from a slow convergence rate due to potential ill-conditioned tensor modes (see also Section 4.3). Moreover, it will allow us to prove a global approximation result showing convergence towards a so-called low-Tucker-rank winning ticket: a subnetwork formed of convolutional layers with a low Tucker rank that well-approximates the original full model.

Let f be a convolutional neural network and let W be a convolutional kernel tensor within f . Consider the problem of minimizing the loss function \mathcal{L} with respect to just W , while maintaining the other parameters fixed. This problem can be equivalently formulated as the differential equation

$$\dot{W}(t) = -\nabla_W \mathcal{L}(W(t)) \quad (5)$$

where, for simplicity, we write the loss as a function of only W and where “dot” denotes the time derivative. When $t \rightarrow \infty$, the solution of (5) approaches the desired minimizer. Now, suppose we parametrize each convolutional layer in a time-dependent Tucker form $W(t) = C(t) \times_{i=1}^4 U_i(t)$. Using standard derivations from dynamical model order reduction literature [26], we derive below the equations for the individual factors $C(t)$ and $U_i(t)$.

To this end, notice that by definition, if $W(t) \in \mathcal{M}_\rho$, then $\dot{W}(t) \in T_{W(t)}\mathcal{M}_\rho$, the tangent space of \mathcal{M}_ρ at $W(t)$. Thus, when $W(t) \in \mathcal{M}_\rho$, (5) boils down to [26]

$$\dot{W}(t) = -P(W(t))\nabla_W \mathcal{L}(W(t)) \quad (6)$$

where $P(W)$ denotes the orthogonal projection onto $T_W\mathcal{M}_\rho$. Note that, for a fixed point $W \in \mathcal{M}_\rho$, $P(W)$ is a linear map defined in terms of the optimization problem

$$P(W) [-\nabla_W \mathcal{L}(W)] = \underset{\delta W \in T_W\mathcal{M}_\rho}{\operatorname{argmin}} \|\delta W + \nabla_W \mathcal{L}(W)\|, \quad (7)$$

where here and henceforth $\|\cdot\|$ denotes the Frobenius norm. Since $\|\cdot\|$ is induced by the inner product $\langle W, Y \rangle = \sum_{i_1, \dots, i_4} W(i_1, \dots, i_4)Y(i_1, \dots, i_4)$, the projection in (7) can be derived by imposing orthogonality with any element of the tangent space. This means that it is possible to derive the ODEs for the projected dynamics by imposing a time-dependent Galerkin condition on the tangent space of \mathcal{M}_ρ , i.e. by imposing the following

$$\langle \dot{W}(t) + \nabla_W \mathcal{L}(W(t)), \delta W \rangle = 0, \quad \forall \delta W \in T_{W(t)}\mathcal{M}_\rho.$$

Using the representation (4) combined with the standard gauge conditions $U_i^\top \delta U_i = 0, \forall \delta U_i \in T_{U_i}\mathcal{S}_i$, for the Stiefel manifold \mathcal{S}_i , we obtain that the projected gradient flow (6) coincides with the coupled matrix-tensor system of ODEs

$$\begin{cases} \dot{U}_i &= -(I - U_i U_i^\top) \operatorname{Mat}_i(\nabla_W \mathcal{L}(W) \times_{j \neq i} U_j^\top) \operatorname{Mat}_i(C)^\dagger, \quad i = 1, \dots, 4 \\ \dot{C} &= -\nabla_W \mathcal{L}(W) \times_{j=1}^4 U_j^\top. \end{cases} \quad (8)$$

where \dagger denotes the pseudoinverse and where we omitted the dependence on t for brevity. Even though (8) describes the dynamics of the individual factors, the equations for each factor are not fully decoupled. In fact, a direct integration of (8) would still require taping the gradients $\nabla_W \mathcal{L}$ with respect to the full convolutional kernel W . Moreover, the presence of the pseudoinverse of the matrices $\operatorname{Mat}_i(C)^\dagger$ adds a stiffness term to the differential equation, making its numerical integration unstable. The presence of this stiff term is actually due to the intrinsic high-curvature of the manifold \mathcal{M}_ρ and is well understood in the dynamic model order reduction community [25, 34, 23, 35, 6, 5]. As observed in [42], an analogous term arises when looking at low-rank matrix parameterizations, and it is responsible for the issue of slow convergence of low-rank matrix training methods which is observed in [51, 22, 42].

To overcome these issues, we make the following key change of variable, inspired by the matrix-based training scheme proposed in [42]. Let $\operatorname{Mat}_i(C)^\top = Q_i S_i^\top$ be the QR decomposition of $\operatorname{Mat}_i(C)^\top$. Note that S_i is a small square invertible matrix of size $r_i \times r_i$. Then, the matrix $K_i = U_i S_i$ has the same size as U_i and spans the same vector space. However, the following key result holds for K_i .

Theorem 1. *Let $W = C \times_{i=1}^4 U_i \in \mathcal{M}_\rho$ be such that (7) holds. Let $\operatorname{Mat}_i(C)^\top = Q_i S_i^\top$ be the QR decomposition of $\operatorname{Mat}_i(C)^\top$ and let $K_i = U_i S_i$. Then,*

$$\dot{K}_i = -\nabla_{K_i} \mathcal{L}(\operatorname{Ten}_i(Q_i^\top) \times_{j \neq i} U_j \times_i K_i) \quad \text{and} \quad \dot{C} = -\nabla_C \mathcal{L}(C \times_{j=1}^4 U_j) \quad (9)$$

where Ten_i denotes “tensorization along mode i ”, i.e. the inverse reshaping operation of Mat_i .

The proof is provided in Appendix B in the supplementary material. The theorem above allows us to simplify Equation (8) obtaining a gradient flow that only depends on the small matrices K_i and the small

core tensor C . Moreover, it allows us to get rid of the stiffness term, as no inversion is now involved in the differential equations. Based on Theorem 1, we formulate in the next section the proposed modified training step for convolutional layers. Notably, by a key basis-augmentation step, we will equip the algorithm with a rank-adjustment step that learns the Tucker rank of the convolutions during training, while maintaining guarantees of descent and approximation of the vanilla full convolutional kernel, as shown by the theoretical analysis in Section 3.2.

3.1 Rank-adaptive Algorithm and implementation details

The training algorithm for convolutional layers in Tucker format is presented in Algorithm 1. Each time we back-propagate through a convolutional layer $W = C \times_{i=1}^4 U_i$, we form the new variable $K_i = U_i S_i$ as in Theorem 1, we integrate the ODE in (10) from $K_i(0) = K_i$ to $K_i(\lambda)$, $\lambda > 0$, and then update the factors U_i by forming an orthonormal basis of the range of $K_i(\lambda)$. In practice, we implement the orthonormalization step via the QR factorization, while we perform the integration of the gradient flow via stochastic gradient descent with momentum and learning rate λ , which coincides with a stable two-step linear multistep integration method [43]. Once all the factors U_i are updated, we back-propagate the core term by integrating the equation for C in (10), using the same approach.

An important feature of the proposed back-propagation step is that the Tucker rank of the new kernel can be adaptively learned with a key basis-augmentation trick: each time we backprop $K_i \in \mathbb{R}^{n_i \times r_i}$, we form an augmented basis \tilde{K}_i by appending the previous U_i to the new $K_i(\lambda)$, $\tilde{K}_i = [K_i | U_i]$. We compute an orthonormal basis $U_i^{\text{new}} \in \mathbb{R}^{n_i \times 2r_i}$ for \tilde{K}_i and we form the augmented $2r_1 \times \dots \times 2r_4$ core $\tilde{C} = C \times_{i=1}^4 (U_i^{\text{new}})^\top U_i$. We then backpropagate the core C integrating (10) starting from $C(0) = \tilde{C}$. Finally, we perform a rank adjustment step by computing the best Tucker approximation of \tilde{C} to a relative tolerance $\tau > 0$. This step corresponds to solving the following optimization (rounding) task:

$$\text{Find } \hat{C} \in \mathcal{M}_{\leq 2\rho} \text{ of smallest rank } \rho' = (r'_1, \dots, r'_4) \text{ such that } \|\tilde{C} - \hat{C}\| \leq \tau \|\tilde{C}\|$$

where $\rho = (r_1, \dots, r_4)$ and $\mathcal{M}_{\leq 2\rho}$ denotes the set of tensors with component-wise Tucker rank lower than 2ρ . In practice, this is done by unfolding the tensor along each mode and computing a truncated SVD of the resulting matrix, as implemented in the `torch` library [48]. The tensor $\hat{C} \in \mathcal{M}_{\rho'}$ is then further decomposed in its Tucker decomposition yielding a factorization $\hat{C} = C' \times_{i=1}^4 U_i' \in \mathcal{M}_{\rho'}$. The parameter τ is responsible for the compression rate of the method, as larger values of τ yield smaller Tucker ranks and thus higher parameter reduction. To conclude, the computed $U_i' \in \mathbb{R}^{2r_i \times r'_i}$ with $r'_i \leq 2r_i$ are then pulled back to the initial dimension of the filter by setting $U_i = U_i^{\text{new}} U_i' \in \mathbb{R}^{n_i \times r'_i}$, and the new core tensor C is then assigned C' .

3.2 Analysis of loss descent and search of winning tickets

In this section, we present our main theoretical results. First, we show that the back-propagation step in Algorithm 1 guarantees descent of the training loss, provided the compression tolerance is not too large. Second, we show that the convolutional filter in compressed Tucker format computed via the rank-adaptive back-propagation step in Algorithm 1 well-approximates the full filter one would obtain by standard training, provided the gradient flow of the loss is, at each step, approximately low-rank. For smooth losses \mathcal{L} , the latter requirement can be interpreted as assuming the existence of a winning ticket of low Tucker rank, i.e. a subnetwork whose convolutions have small Tucker rank and that well-approximates the performance of the large initial net. In this sense, our second result shows that, if a low-Tucker-rank winning ticket exists, then the proposed Tucker-tensor flow (10) approaches it. For the sake of brevity, some statements here are formulated informally. All proofs and details are provided in Appendix C in the supplementary material.

Suppose that for each convolution W , the gradient $\nabla_W \mathcal{L}$, as a function of W , is locally bounded and Lipschitz, i.e. $\|\nabla_W \mathcal{L}(Y)\| \leq L_1$ and $\|\nabla_W \mathcal{L}(Y_1) - \nabla_W \mathcal{L}(Y_2)\| \leq L_2 \|Y_1 - Y_2\|$ around W . Then,

Theorem 2. *Let $W(\lambda) = C \times_{j=1}^4 U_j$ be the Tucker low-rank tensor obtained after one training iteration using Algorithm 1 and let $W(0)$ be the previous point. Assuming the one-step integration from 0 to λ is done exactly, it holds $\mathcal{L}_W(W(\lambda)) \leq \mathcal{L}_W(W(0)) - \alpha\lambda + \beta\tau$, where $\alpha, \beta > 0$ are constants independent of λ and τ , and where \mathcal{L}_W denotes the loss as a function of only W .*

Algorithm 1: TDLRT: Dynamical Low-Rank Training of convolutions in Tucker format.

Input : Convolutional filter $W \sim n_1 \times n_2 \times n_3 \times n_4$;
Initial low-rank factors $C \sim r_1 \times \dots \times r_4$; $U_i \sim n_i \times r_i$;
adaptive: Boolean flag that decides whether or not to dynamically update the ranks;
 τ : singular value threshold for the adaptive procedure.

```
1 for each mode  $i$  do
2    $Q_i S_i^\top \leftarrow$  QR decomposition of  $\text{Mat}_i(C)^\top$ 
3    $K_i \leftarrow U_i S_i$ 
4    $K_i \leftarrow$  descent step; direction  $\nabla_{K_i} \mathcal{L}(\text{Ten}_i(Q_i^\top) \times_{j \neq i} U_j \times_i K_i)$ ; starting point  $K_i$ 
5   if adaptive then                                     /* Basis augmentation step */
6     |  $K_i \leftarrow [K_i \mid U_i]$ 
7     |  $U_i^{\text{new}} \leftarrow$  orthonormal basis for the range of  $K_i$ 
8    $\tilde{C} \leftarrow C \times_{i=1}^4 (U_i^{\text{new}})^\top U_i$ 
9    $C \leftarrow$  descent step; direction  $\nabla_C \mathcal{L}(\tilde{C} \times_{i=1}^4 U_i^{\text{new}})$ ; starting point  $\tilde{C}$ 
10 if adaptive then                                       /* Rank adjustment step */
11   |  $(\tilde{C}, U_1, \dots, U_4) \leftarrow$  Tucker decomposition of  $\tilde{C}$  up to relative error  $\tau$ 
12   |  $U_i \leftarrow U_i^{\text{new}} U_i$ , for  $i = 1, \dots, 4$ 
13 else
14   |  $U_i \leftarrow U_i^{\text{new}}$ , for  $i = 1, \dots, 4$ 
```

Theorem 3. For an integer k , let $t = k\lambda$, and let $W(t)$ be the full convolutional kernel, solution of (5) at time t . Let $C(t), \{U_i(t)\}_i$ be the Tucker core and factors computed after k training steps with Algorithm 1, where the one-step integration from 0 to λ is done exactly. Finally, assume that for any Y in a neighborhood of $W(t)$, the gradient flow $-\nabla \mathcal{L}_W(Y)$ is “ ε -close” to $T_Y \mathcal{M}_p$. Then,

$$\|W(t) - C(t) \times_{j=1}^4 U_j(t)\| \leq c_1 \varepsilon + c_2 \lambda + c_3 \tau / \lambda$$

where the constants c_1, c_2 and c_3 depend only on L_1 and L_2 .

In particular, both bounds in the above theorems do not depend on the higher-order singular values of the exact nor the approximate solution, which shows that the method does not suffer instability and slow convergence rate due to potential ill-conditioning (small higher-order singular values).

4 Experiments

In the following, we conduct a series of experiments to evaluate the performance of the proposed method, as compared to the full baseline, the matrix DLRT algorithm [42], and so-called “vanilla” low-rank models. The vanilla strategies perform the obvious low-rank approach: each layer is parametrized by a low-rank factorization and training is implemented by alternate descent steps over each of the low-rank parameters. The three parametrizations we use are the Canonic-Polyadic decomposition (Vanilla CP), as done in e.g. [29, 45, 1, 41], the Tucker decomposition (Vanilla Tucker) as in e.g. [28, 24], and the standard matrix factorization after matricization of the layers (Vanilla Matrix), as done in e.g. [21, 31, 51, 22]. All the experiments are conducted using an Nvidia RTX 3090 GPU as computing hardware, and the code is available in the supplementary material.

4.1 Compression Performance

The compression performance of TDLRT is evaluated on the CIFAR-10 dataset, containing 60K RGB images of 10 classes. No data augmentation is used and all methods are trained using a batch size of 128 for 70 epochs each, with 20 randomly sampled weight initializations of all trainable parameters, as done in [51, 22], using Equation (2). All the vanilla methods are trained with the SGD optimizer; the learning rate and momentum are chosen as above. The fixed low-ranks \hat{r} of each tensor mode of the baseline methods is determined by a parameter κ , i.e. we set $\hat{r} = \kappa r_{\max}$. The proposed TDLRT method employs

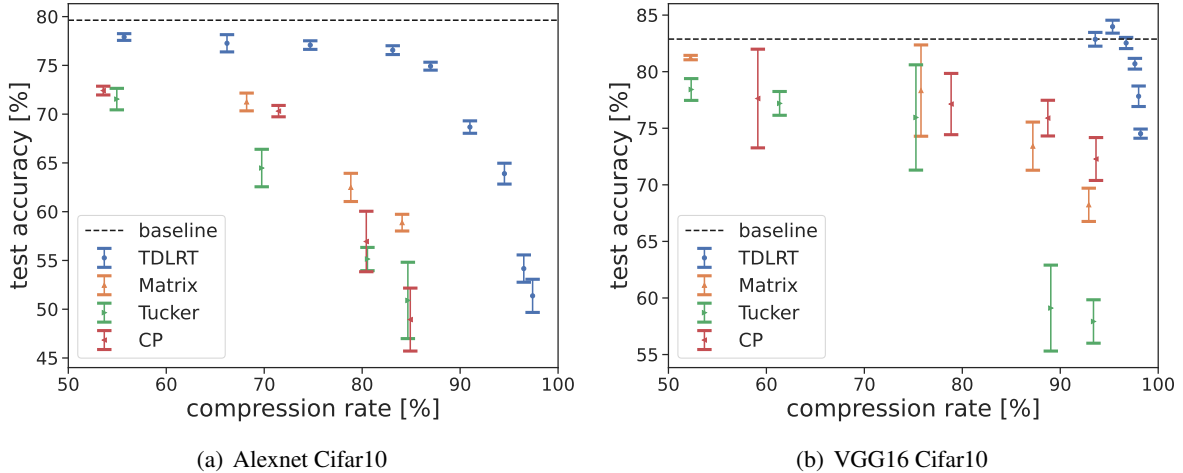


Figure 1: Comparison of Vanilla compression with different tensor formats with the proposed TDLRT method. Mean and standard deviation of 20 weight initializations are displayed. TDLRT achieves higher compression rates at higher accuracy with lower variance between initializations.

Table 1: Comparison of the best-performing compression rates for different methods on the CIFAR10 benchmark at Alexnet and VGG16. TDLRT significantly outperforms vanilla methods and matrix-valued dynamic methods [42] in terms of accuracy and compression rate.

method	VGG16			Alexnet		
	test acc.[%]	compression rate [%]		test acc.[%]	compression rate [%]	
		eval	train		eval	train
Baseline	82.88 ± 0.23	0.0		79.63 ± 0.30	0	
TDLRT	83.97 ± 0.57	95.34	69.92	76.56 ± 0.45	83.12	29.82
Matrix DLRT [42]	82.58 ± 0.21	83.22	74.30	67.74 ± 0.19	71.57	55.51
Vanilla Tucker	77.19 ± 1.05	61.34		64.47 ± 1.92	69.74	
Vanilla Matrix	73.41 ± 2.12	87.20		71.24 ± 0.91	68.20	
Vanilla CP	77.13 ± 2.70	78.85		70.31 ± 0.58	71.46	

Algorithm 1, where SGD is used for each K -step and C -step with momentum and learning rate as above. Dynamic compression during training is governed by the singular value threshold τ , see Section 3.1.

Figure 1 compares the test accuracy and compression of TDLRT to the vanilla training and the full baseline, where mean and standard deviation of each data point is displayed. TDLRT achieves higher compression rates at higher accuracy with lower variance between weight initializations than the vanilla methods. In the case of the VGG16 benchmark, TDLRT is able to maintain baseline accuracy for compression rates over 90% and exceeds the baseline on average for $\tau = 0.03$, i.e. 95.3% compression. Alexnet has 16.8% of the parameters of VGG16, thus compression is naturally harder to achieve. Yet, TDLRT outperforms the vanilla methods and remains close to baseline performance. Remark, that the robustness of the low-rank TDLRT integrator results in less variance between weight initializations. The loss-descent guarantee of Theorem 2 ensures successful training even for compressed networks, and the accuracy result of Theorem 3 enables higher compression rates than the vanilla approaches with close to baseline performance.

Table 1 shows a comparison of the best-performing compression between various vanilla methods as well as Tucker and matrix-valued dynamical low-rank compression algorithms in the CIFAR benchmark for Alexnet and VGG16. TDLRT outperforms the matrix-valued dynamical low-rank compression of convolutions, due to the higher flexibility of the Tucker format, where compression along each tensor mode individually is possible. We also remark that CP decomposition is not suited for dynamical low-rank training due to its lack of a manifold structure.

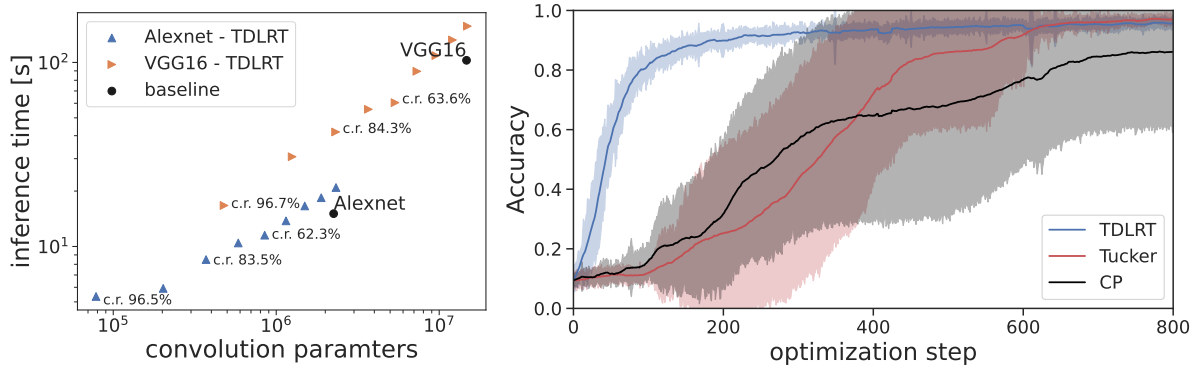


Figure 2: Left panel: Computational footprint of low-rank convolutions. TDLRT surpasses the baseline performance for meaningful compression rates. Right panel: Convergence behavior of Lenet5 on MNIST dataset in the case of an initial overestimation of the rank, with exponentially decaying singular values. Mean and standard deviation (shaded area) over 10 random initializations.

4.2 Computational Performance

The computational performance in inference and training of convolutional layers in Tucker decomposition is dependent on their current tensor ranks, see Section 2.1. We evaluate the inference time of 120K RGB images and memory footprint of VGG and AlexNet in Tucker factorization as used in Algorithm 1 and compare them to the non-factorized baseline models in Figure 2. As a result, for realistic compression rates, see also Figure 1, the computational footprint of TDLRT is significantly lower than the corresponding baseline model.

4.3 Robustness of the Optimization

We compare TDLRT, the vanilla tucker, and the vanilla CP method in the MNIST test case with above described optimizer, learning rate, momentum and batch size, over the corresponding optimization steps of the methods for Lenet5. In the case of TDLRT, an optimization step denotes the evaluation of Algorithm 1 for all convolutional layers for one batch of training data, in the case of the vanilla methods, a standard gradient descent batch update for all factors of the tensor decompositions of all layers. All linear layers of the network are trained with a traditional gradient descent update and are not compressed. In this experiment, we initialize the network weights to simulate a scenario where the rank is overestimated. To this end, we employ spectral initialization with singular values decaying exponentially with powers of ten. Integrating the low-rank gradient flow with the TDLRT Algorithm 1, leads to faster and more robust convergence rates of the network training process compared to vanilla methods, as shown in Figure 2.

5 Discussion and limitations

To conclude, this work introduces a training algorithm that adaptively prunes convolutional layers during training, yielding a significant reduction in computational and memory costs. The construction of the method allows rigorous proofs of a robust error bound and robust descent direction, i.e., error and descent are not affected by the intrinsic high curvature of the low-rank manifold. Numerical experiments validate the provided theoretical results and show significantly faster and more robust convergence compared to vanilla approaches. Further, TDLRT offers two major significant enhancements: It avoids inefficient and computationally costly matricizations of large tensors, and it adaptively learns the Tucker ranks increasing the approximation expressivity of the low-rank network.

Despite its numerous properties, TDLRT and pruning methods for convolutional layers in general face several challenges that require further investigation, as we overview below.

First, the proposed training algorithm relies on the hypothesis that well-performing spectrally-sparse structures are hidden in the reference network. Moreover, low-rank neural networks introduce spurious local minima arising from parametrization’s invariance and artificially increase the effective width leading

to the known fact that pruning deep neural networks during training can slow down convergence [2]. We also note that, in the terminology of [44], TDLRT does not aim at reducing activation costs and instead reduces training and inference costs that correspond to model parameters and the optimizer. Finally, an efficient compression requires an appropriate strategy to choose the tolerance parameter τ combined with a computationally efficient tensor rounding algorithm. Even if HOSVD provides quasi-optimal approximation bounds, the application of alternative techniques based on, e.g., randomization, may certainly lead to a boost in computational performance. On the other hand, the approximation error induced by randomized algorithms requires to be properly treated and controlled to preserve TDLRT’s theoretical guarantees.

A Additional experiments

In this section we are presenting all the additional results that for space reasons we left out of the main manuscript.

In particular, Tab.4 reports the results of Lenet5 on MNIST dataset, in comparison with the same approaches presented in the first part of the paper. Additionally, in Tab.3 some results using Lenet5 on Fashion-Mnist are reported. Table5 instead reports additional results using VGG16 and Alexnet on Cifar10. In particular, we present a table of results comparing our proposal with other approaches, both using Lenet5 on MNIST and Fashion-Mnist datasets. Moreover, Tab.2 contains the Tucker ranks of some of the runs of Alexnet presented in section4.1.

All the test cases were run with the rank adaptive version of the integrator, and in all the reported results we include mean and standard deviation over five random initializations. No data augmentation is used and all methods are trained for 70 epochs using a batch size of 128. All method are trained using the SGD optimizer, with a starting learning rate of 5×10^{-2} with a scheduler that is reducing it by a factor of 10 whenever validation loss reaches a plateau. Polyak momentum was 0.1 for all layers but batch normalizations, in which it was set to 0.9.

Results in Tab.4 and Tab.3 show that for easier tasks both our proposal and the other methods are performing in a comparable way. However, for more complicated datasets and architectures like Cifar10 on VGG16 and Alexnet, results in Tab.5 show that our proposal consistently gets better results than all the methods under comparison at parity of compression.

Table 2: Reproduction of the results of Alexnet on Cifar10. The results are averaged across 5 random initialization. The ranks reported refer to the Tucker ranks of each convolutional layer.

Alexnet Cifar10 ranks			
	test acc.[%]	layers’ ranks	test compression rate [%]
Baseline	79.63 ± 0.30	$[64, 3, 3, 3]$ $[192, 64, 3, 3]$ $[384, 192, 3, 3]$ $[256, 384, 3, 3]$ $[256, 256, 3, 3]$	0.0
TDLRT $\tau = 0.6$	76.26 ± 0.88	$[25, 3, 3, 3]$ $[76, 25, 3, 3]$ $[153, 76, 3, 3]$ $[102, 153, 3, 3]$ $[102, 102, 3, 3]$	74
TDLRT $\tau = 0.7$	73.08 ± 0.44	$[19, 3, 3, 3]$ $[57, 19, 3, 3]$ $[115, 57, 3, 3]$ $[76, 115, 3, 3]$ $[76, 76, 3, 3]$	83.5

Table 3: Lenet5 on Fashion-Mnist dataset.

Lenet5 FASHION MNIST			
method	test acc.[%]	convolutions compression rate	
	(to baseline)	eval[%]	train[%]
Baseline	90.86 ± 0.10	0.0	0.0
TDLRT $\tau = 0.1$	87.42 ± 0.73	94.42 ± 0.17	64.10 ± 3.13
TDLRT $\tau = 0.15$	88.89 ± 0.19	96.92 ± 0.11	92.58 ± 0.71
TDLRT $\tau = 0.2$	88.86 ± 0.11	97.00 ± 0.05	93.14 ± 0.05
TDLRT $\tau = 0.3$	88.71 ± 0.04	97.10 ± 0.02	94.20 ± 0.01
Vanilla CP	89.36 ± 0.16	96.81	96.81
Vanilla Tucker	89.14 ± 0.21	96.80	96.80
Vanilla Matrix	87.47 ± 0.15	91.88	91.88

Table 4: Lenet5 on MNIST dataset

Lenet5 MNIST			
method	test acc.[%]	convolutions compression rate	
	(to baseline)	eval[%]	train[%]
Baseline	98.14 ± 0.02	0.0	0.0
TDLRT $\tau = 0.15$	97.54 ± 0.27	93.76 ± 0.52	54.02 ± 7.60
TDLRT $\tau = 0.2$	97.80 ± 0.08	96.13 ± 0.26	84.64 ± 3.09
TDLRT $\tau = 0.3$	97.83 ± 0.11	96.52 ± 0.16	89.83 ± 1.56
Vanilla CP	97.56 ± 0.16	99.35	99.35
Vanilla Tucker	97.97 ± 0.12	96.52	93.51
Vanilla Matrix	97.53 ± 0.19	93.40	93.40

B Proof of Theorem 1

Theorem. Let $W = C \times_{i=1}^4 U_i \in \mathcal{M}_\rho$ be such that (7) holds. Let $\text{Mat}_i(C)^\top = Q_i S_i^\top$ be the QR decomposition of $\text{Mat}_i(C)^\top$ and let $K_i = U_i S_i$. Then,

$$\dot{K}_i = -\nabla_{K_i} \mathcal{L}(\text{Ten}_i(Q_i^\top) \times_{j \neq i} U_j \times_i K_i) \quad \text{and} \quad \dot{C} = -\nabla_C \mathcal{L}(C \times_{j=1}^4 U_j) \quad (10)$$

where Ten_i denotes “tensorization along mode i ”, i.e. the inverse reshaping operation of Mat_i .

Proof. The proof follows the path first suggested in [33, §4], i.e., the quantity V_i defined next is frozen in time: $\dot{V}_i = 0$. A detailed derivation of the matrix-tensor equations for K_i and C is beyond the scope of the present work and it is provided in [26, 34, 35, 8, 7].

We begin recalling the evolution equations for the factors of the projected gradient flow (6):

$$\begin{cases} \dot{U}_i &= -(I - U_i U_i^\top) \text{Mat}_i(\nabla_W \mathcal{L}(W) \times_{j \neq i} U_j^\top) \text{Mat}_i(C)^\dagger, \quad i = 1, \dots, 4 \\ \dot{C} &= -\nabla_W \mathcal{L}(W) \times_{j=1}^4 U_j^\top. \end{cases}$$

where \dagger denotes the pseudoinverse. We assume that the tensor W admits a differentiable Tucker tensor representation, i.e., $W(t) = C(t) \times_{i=1}^4 U_i(t) \in \mathcal{M}_\rho$ for $t \in [0, \lambda]$ satisfying the associated gradient-flow tensor differential equation

$$\dot{W}(t) = -\nabla_W(t) \mathcal{L}(W(t)).$$

For sake of brevity, the parameter is going to be omitted. Next, we perform a QR-factorization

$$\text{Mat}_i(C)^\top = Q_i S_i^\top.$$

Thus, we observe that the matrix $\text{Mat}_i(W)$ admits an SVD-like decomposition as follows

$$\text{Mat}_i(W) = U_i S_i V_i^\top \quad \text{with} \quad V_i^\top := Q_i^\top \bigotimes_{j \neq i} U_j^\top,$$

Table 5: VGG16 and Alexnet on Cifar10 dataset.

		Cifar10		
method		test acc.[%] (to baseline)	compression rate	
			eval[%]	train[%]
VGG16	Baseline	82.88 ± 0.23%	0.0%	
	TDLRT $\tau = 0.02$	82.86 ± 1.6	93.57 ± 0.12	50.25 ± 1.16
	TDLRT $\tau = 0.03$	83.97 ± 0.57	95.34 ± 0.20	69.92 ± 2.09
	TDLRT $\tau = 0.04$	82.25 ± 0.49	96.71 ± 0.22	84.25 ± 2.12
	TDLRT $\tau = 0.05$	81.04 ± 0.49	97.40 ± 0.10	90.33 ± 0.85
	TDLRT $\tau = 0.06$	80.70 ± 0.47	97.62 ± 0.04	92.38 ± 0.46
	TDLRT $\tau = 0.1$	77.80 ± 0.90	98.01 ± 0.08	95.51 ± 0.53
	TDLRT $\tau = 0.15$	74.52 ± 1.04	98.23 ± 0.02	96.67 ± 0.12
	Vanilla CP $\kappa = 0.95$	72.28 ± 1.89	93.64	
	Vanilla CP $\kappa = 0.9$	75.89 ± 1.57	88.73	
	Vanilla CP $\kappa = 0.8$	77.13 ± 2.71	78.86	
	Vanilla CP $\kappa = 0.6$	77.62 ± 4.36	59.12	
	Vanilla Tucker $\kappa = 0.95$	57.92 ± 1.91	93.39	
	Vanilla Tucker $\kappa = 0.9$	59.10 ± 3.79	89.03	
	Vanilla Tucker $\kappa = 0.8$	75.95 ± 4.65	75.26	
	Vanilla Tucker $\kappa = 0.6$	77.19 ± 1.05	61.34	
	Vanilla Tucker $\kappa = 0.4$	78.42 ± 0.96	52.32	
	Vanilla Matrix $\kappa = 0.95$	68.23 ± 1.47	92.90	
	Vanilla Matrix $\kappa = 0.9$	73.41 ± 2.12	87.20	
	Vanilla Matrix $\kappa = 0.8$	78.32 ± 4.03	75.78	
	Vanilla Matrix $\kappa = 0.6$	81.25 ± 0.19	52.26	
	DLRT	82.58 ± 0.20	83.22	74.3
	Alexnet	Baseline	79.63 ± 0.30	0.0
TDLRT $\tau = 0.06$		76.56 ± 0.45	83.12 ± 0.80	29.82 ± 8.72
TDLRT $\tau = 0.1$		74.92 ± 0.40	86.98 ± 0.08	72.42 ± 0.98
TDLRT $\tau = 0.15$		71.34 ± 0.31	91.78 ± 0.09	78.60 ± 0.73
Vanilla CP $\kappa = 0.95$		48.93 ± 3.23	84.91	
Vanilla CP $\kappa = 0.9$		56.94 ± 3.10	80.42	
Vanilla CP $\kappa = 0.8$		70.31 ± 0.58	71.46	
Vanilla CP $\kappa = 0.7$		72.41 ± 0.44	53.56	
Vanilla Tucker $\kappa = 0.95$		50.90 ± 3.91	84.66	
Vanilla Tucker $\kappa = 0.9$		55.14 ± 1.19	80.53	
Vanilla Tucker $\kappa = 0.8$		64.47 ± 1.92	69.74	
Vanilla Tucker $\kappa = 0.6$		71.54 ± 1.10	54.95	
Vanilla Matrix $\kappa = 0.95$		58.87 ± 0.85	84.07	
Vanilla Matrix $\kappa = 0.9$		62.48 ± 1.45	78.84	
Vanilla Matrix $\kappa = 0.8$		71.24 ± 0.91	68.20	
DLRT		67.74 ± 0.19	71.57	55.5

where the matrix Q_i possess orthonormal columns, i.e., $Q_i^\top Q_i = I$. We introduce the quantity

$$K_i := U_i S_i \quad \text{where} \quad S_i = \text{Mat}_i(C) Q_i.$$

By construction, we observe that

$$S_i = U_i^\top \text{Mat}_i(W) V_i.$$

The tiny matrix S_i satisfies the following differential equation

$$\begin{aligned}
\dot{S}_i &= \dot{U}_i^\top \text{Mat}_i(W)V_i + U_i^\top \text{Mat}_i(\dot{W})V_i + U_i^\top \text{Mat}_i(W)\dot{V}_i \\
&= \underbrace{(\dot{U}_i^\top U_i)}_{=0} S_i V_i^\top V_i + U_i^\top \text{Mat}_i(\dot{W})V_i + U_i^\top \text{Mat}_i(W) \underbrace{\dot{V}_i}_{=0} \\
&= -U_i^\top \text{Mat}_i(\nabla_W \mathcal{L})V_i.
\end{aligned}$$

The first null identity follows from the gauge condition on U_i . The second null identity follows by the initial assumption $\dot{V}_i = 0$. Therefore, the matrix K_i satisfies the differential equation

$$\begin{aligned}
\dot{K}_i &= (U_i \dot{S}_i) \\
&= \dot{U}_i S_i + U_i \dot{S}_i \\
&= -(I - U_i U_i^\top) \text{Mat}_i(\nabla_W \mathcal{L} \times_{j \neq i} U_j^\top) \text{Mat}_i(C)^\dagger S_i - U_i U_i^\top \text{Mat}_i(\nabla_W \mathcal{L})V_i \\
&= (U_i U_i^\top - I) \text{Mat}_i(\nabla_W \mathcal{L} \times_{j \neq i} U_j^\top) Q_i - U_i U_i^\top \text{Mat}_i(\nabla_W \mathcal{L})V_i \\
&= (U_i U_i^\top - I) \text{Mat}_i(\nabla_W \mathcal{L}) \cdot \left(\otimes_{j \neq i} U_j \right) Q_i - U_i U_i^\top \text{Mat}_i(\nabla_W \mathcal{L})V_i \\
&= (U_i U_i^\top - I) \text{Mat}_i(\nabla_W \mathcal{L})V_i - U_i U_i^\top \text{Mat}_i(\nabla_W \mathcal{L})V_i \\
&= -\text{Mat}_i(\nabla_W \mathcal{L})V_i.
\end{aligned} \tag{11}$$

To conclude, we set $Z = K_i V_i^\top$ and let $W = \text{Ten}_i(K_i V_i^\top) = \text{Ten}_i(Z)$. We obtain

$$\nabla_{K_i} \mathcal{L}(W) = \nabla_Z \mathcal{L}(\text{Ten}_i(Z)) \nabla_Z K_i = \nabla_Z \mathcal{L}(\text{Ten}_i(Z))V_i.$$

where we remind that $V_i^\top V_i = I$. Hence

$$\text{Mat}_i(\nabla_W \mathcal{L}(W))V_i = \nabla_Z \mathcal{L}(\text{Ten}_i(Z))V_i = \nabla_{K_i} \mathcal{L}(W). \tag{12}$$

The first K_i -differential equation is then obtained combining (13) and (12)

$$\dot{K}_i = -\text{Mat}_i(\nabla_W \mathcal{L})V_i = -\nabla_{K_i} \mathcal{L} \left(\text{Ten}_i(K_i V_i^\top) \right). \tag{13}$$

The right hand side can be further reduced using standard tensorization formulas[27]

$$\text{Ten}_i(K_i V_i^\top) = \text{Ten}_i(Q_i^\top) \times_{j \neq i} U_j \times_i K_i.$$

The second differential equations follows by observing that

$$\nabla_W \mathcal{L} = \nabla_C \mathcal{L} \times_i U_i + \sum_j \mathcal{L} \times_j \dot{U}_j \times_{i \neq j} U_i.$$

The tensor C satisfies the differential equation

$$\begin{aligned}
\dot{C} &= -\nabla_W \mathcal{L}(W) \times_i U_i^\top \\
&= -\nabla_C \mathcal{L}(W) \times_i U_i \times_i U_i^\top \\
&= -\nabla_C \mathcal{L}(W) \times_i \underbrace{U_i^\top U_i}_{=I} \\
&= -\nabla_C \mathcal{L}(C \times_i U_i).
\end{aligned}$$

where the extra terms disappear due to the imposed gauge conditions $U_i^\top \dot{U}_i = 0$. \square

C Proofs of descent and approximation theorems

The following Theorems and Lemmas extend the matrix result available in [42] to tensors in Tucker format. The core elements of the proofs have been first provided in [5].

Theorem. Let $W(\lambda) = C \times_{j=1}^4 U_j$ be the Tucker low-rank tensor obtained after one training iteration using Algorithm 1 and let $W(0)$ be the previous point. Then, for a small enough learning rate λ , it holds $\mathcal{L}_W(W(\lambda)) \leq \mathcal{L}_W(W(0)) - \alpha\lambda + \beta\tau$, where $\alpha, \beta > 0$ are constants independent of λ and τ , and where \mathcal{L}_W denotes the loss as a function of only W .

Proof. Let $\widehat{W}(t) = \widehat{C}(t) \times_i \widehat{U}_i^1$. Here, $\widehat{W}(t)$ and $\widehat{C}(t)$ denote the augmented solutions for $t \in [0, \lambda]$ arising from the intermediate steps of the TDLRT Algorithm 1. We observe that

$$\begin{aligned} \frac{d}{dt} \mathcal{L}(\widehat{W}(t)) &= \langle \nabla \mathcal{L}(\widehat{W}(t)), \dot{\widehat{W}}(t) \rangle \\ &= \langle \nabla \mathcal{L}(\widehat{W}(t)), \dot{\widehat{C}}(t) \times_i \widehat{U}_i^1 \rangle \\ &= \langle \nabla \mathcal{L}(\widehat{W}(t)) \times_i \widehat{U}_i^{1,\top}, \dot{\widehat{C}}(t) \rangle \\ &= \langle \nabla \mathcal{L}(\widehat{W}(t)) \times_i \widehat{U}_i^{1,\top}, -\nabla \mathcal{L}(\widehat{W}(t)) \times_i \widehat{U}_i^{1,\top} \rangle = -\|\nabla \mathcal{L}(\widehat{W}(t)) \times_i \widehat{U}_i^{1,\top}\|^2. \end{aligned}$$

If we define $\alpha := \min_{0 \leq \tau \leq 1} \|\nabla \mathcal{L}(\widehat{W}(\tau\lambda)) \times_i \widehat{U}_i^{1,\top}\|^2$, it follows that for $t \in [0, \lambda]$

$$\frac{d}{dt} \mathcal{L}(\widehat{W}(t)) \leq -\alpha. \quad (14)$$

Integrating (14) from $t = 0$ until $t = \lambda$, we obtain

$$\mathcal{L}(\widehat{W}(\lambda)) \leq \mathcal{L}(\widehat{W}(0)) - \alpha\lambda.$$

Because the augmented subspaces \widehat{U}_i contain by construction the range and co-range of the initial value, we have that $\widehat{W}(0) = W(0)$. Furthermore, the truncation is such that $\|W(\lambda) - \widehat{W}(\lambda)\| \leq \tau$. Therefore

$$\mathcal{L}(W(\lambda)) \leq \mathcal{L}(\widehat{W}(\lambda)) + \beta\tau$$

where $\beta = \max_{0 \leq \tau \leq 1} \|\nabla \mathcal{L}(\tau W(\lambda) + (1 - \tau)\widehat{W}(\lambda))\|$. \square

The following Lemma is needed to derive a global error bound for the TuckerDLRT algorithm. It extends the matrix results of [42, Appendix].

Lemma 1. *The following estimate holds*

$$\|W(\lambda) - W(\lambda) \times_j U_j(\lambda) U_j(\lambda)^\top\| \leq \Theta = \mathcal{O}(h(h + \epsilon)),$$

where the hidden constants depend only on L_1 and L_2 .

Proof. It has been shown in [42, Appendix] that there exists a constant $\theta \propto \mathcal{O}(h(h + \epsilon))$ such that

$$\|U_j U_j^\top \text{Mat}_j(W(\lambda)) - \text{Mat}_j(W(\lambda))\| \leq \theta \quad \forall j = 1, \dots, 4,$$

where the value θ has been shown to depend only on the constants L_1, L_2 and λ . Let $d = 4$, the proof of the Lemma follows a recursive constructive argument

$$\begin{aligned} &\|W(\lambda) - W(\lambda) \times_j^d U_j(\lambda) U_j(\lambda)^\top\| \\ &\leq \|W(\lambda) - W(\lambda) \times_j^{d-1} U_j(\lambda) U_j(\lambda)^\top\| + \|W(\lambda) \times_j^{d-1} U_j(\lambda) U_j(\lambda)^\top - W(\lambda) \times_j^d U_j(\lambda) U_j(\lambda)^\top\| \\ &\leq \|W(\lambda) - W(\lambda) \times_j^{d-1} U_j(\lambda) U_j(\lambda)^\top\| + \|(W(\lambda) \times_d U_d(\lambda) U_d(\lambda)^\top - W(\lambda)) \times_j^{d-1} U_j(\lambda) U_j(\lambda)^\top\| \\ &\leq \|W(\lambda) - W(\lambda) \times_j^{d-1} U_j(\lambda) U_j(\lambda)^\top\| + \|W(\lambda) \times_d U_d(\lambda) U_d(\lambda)^\top - W(\lambda)\| \\ &\leq \|W(\lambda) - W(\lambda) \times_j^{d-1} U_j(\lambda) U_j(\lambda)^\top\| + \theta. \end{aligned}$$

The conclusion is obtained iterating the provided argument. \square

Theorem 4. *For an integer k , let $t = k\lambda$, and let $W(t)$ be the full convolutional kernel, solution of (5) at time t . Let $C(t), \{U_i(t)\}_i$ be the Tucker core and factors computed after k training steps with Algorithm 1, where the one-step integration from 0 to λ is done exactly. Finally, assume that for any Y in a neighborhood of $W(t)$, the gradient flow $-\nabla \mathcal{L}_W(Y)$ is “ ε -close” to \mathcal{M}_ρ . Then,*

$$\|W(t) - C(t) \times_{j=1}^4 U_j(t)\| \leq c_1 \varepsilon + c_2 \lambda + c_3 \tau / \lambda$$

where the constants c_1, c_2 and c_3 depend only on L_1 and L_2 .

Proof. Let $d = 4$. First, we provide a bound for the local error, i.e., the error obtained after one training epoch. If we apply Lemma 1, we obtain that

$$\begin{aligned} & \|W(\lambda) - C(\lambda) \times_{j=1}^d U_j(\lambda)\| \\ & \leq \|W(\lambda) - W(\lambda) \times_{j=1}^d U_j(\lambda) U_j(\lambda)^\top\| + \|W(\lambda) \times_{j=1}^d U_j(\lambda) U_j(\lambda)^\top - C(\lambda) \times_{j=1}^d U_j(\lambda)\| \\ & \leq \Theta + \left\| \left(W(\lambda) \times_{j=1}^d U_j(\lambda)^\top - C(\lambda) \right) \times_{j=1}^d U_j(\lambda) \right\| \\ & \leq \Theta + \|W(\lambda) \times_{j=1}^d U_j(\lambda)^\top - C(\lambda)\|. \end{aligned}$$

It suffices to study the latter term. For $t \in [0, \lambda]$, we define the quantity

$$\tilde{C}(t) := W(t) \times_{j=1}^d U_j(\lambda)^\top$$

It satisfies the differential initial value problem

$$\dot{\tilde{C}} = -\nabla_W \mathcal{L}(W) \times_{j=1}^d U_j(\lambda)^\top, \quad C(0) = W(0) \times_{j=1}^d U_j(\lambda)^\top.$$

The term $W(t)$ can be written as a perturbation of \tilde{C}

$$W(t) = \tilde{C} \times_{j=1}^d U_j(\lambda) + R(t),$$

where

$$R(t) = W(t) - W(t) \times_{j=1}^d U_j(\lambda) U_j(\lambda)^\top.$$

Then, we observe that

$$\|W(t) - W(\lambda)\| \leq \int_0^\lambda \|\dot{W}(s)\| ds = \int_0^\lambda \|\nabla_W \mathcal{L}(W(s))\| ds \leq C_1 \lambda.$$

The remainder can be estimated as follow

$$\|R(t)\| \leq \|R(t) - R(\lambda)\| + \|R(\lambda)\| \leq 2L_1 \lambda + 2\Theta.$$

Furthermore, the full gradient can be re-written as

$$\nabla_W \mathcal{L}(W(t)) = \nabla_W \mathcal{L}(\tilde{C}(t) \times_{j=1}^d U_j(\lambda) + R(t)) = \nabla_W \mathcal{L}(\tilde{C}(t) \times_{j=1}^d U_j(\lambda)) + D(t),$$

where the defect $D(t)$ is defined as

$$D(t) := \nabla_W \mathcal{L}(\tilde{C}(t) \times_{j=1}^d U_j(\lambda) + R(t)) - \nabla_W \mathcal{L}(\tilde{C}(t) \times_{j=1}^d U_j(\lambda)).$$

Because of the Lipschitz assumption, we have that

$$\|D(t)\| \leq L_2 \|R(t)\| \leq 2L_2(L_1 \lambda + \Theta).$$

Next, we compare the two differential equations

$$\begin{cases} \dot{\tilde{C}}(t) = -\nabla_W \mathcal{L}(\tilde{C}(t) \times_{j=1}^d U_j) \times_{j=1}^d U_j^\top + D(t), \\ \dot{C}(t) = -\nabla_W \mathcal{L}(C(t) \times_{j=1}^d U_j) \times_{j=1}^d U_j^\top, \end{cases}$$

where $C(0) = \tilde{C}(0)$, by construction. The solution $C(\lambda)$ of the second tensor-differential equation coincide with the solution of the last training step of the TuckerDLRT algorithm. The first differential equation has been constructed such that its solution is $\tilde{C}(\lambda) = W(\lambda) \times_j U_j^\top$. Therefore, the study of the local error follows by a direct application of the Gronwall inequality

$$\|C(\lambda) - \tilde{C}(\lambda)\| \leq \exp(C_2 \lambda) 2L_2(L_1 \lambda + \Theta) \lambda.$$

To conclude, the global error in the training epochs follows by using the Lipschitz continuity of the gradient-flow: We move from the local error in time to the global error in time by a standard ODEs argument of Lady Windermere's fan [53, §II.3]. \square

References

- [1] M. Astrid and S.-I. Lee. Cp-decomposition with tensor power method for convolutional neural networks compression. In *2017 IEEE International Conference on Big Data and Smart Computing (BigComp)*, pages 115–118, 2017.
- [2] B. Bah, H. Rauhut, U. Terstiege, and M. Westdickenberg. Learning deep linear neural networks: Riemannian gradient flows and convergence to global minimizers. *Inf. Inference*, 11(1):307–353, 2022.
- [3] B. Baker, I. Akkaya, P. Zhokov, J. Huizinga, J. Tang, A. Ecoffet, B. Houghton, R. Sampedro, and J. Clune. Video pretraining (vpt): Learning to act by watching unlabeled online videos. *Advances in Neural Information Processing Systems*, 35:24639–24654, 2022.
- [4] D. Blalock, J. J. Gonzalez Ortiz, J. Frankle, and J. Gutttag. What is the state of neural network pruning? *Proceedings of machine learning and systems*, 2:129–146, 2020.
- [5] G. Ceruti, J. Kusch, and C. Lubich. A rank-adaptive robust integrator for dynamical low-rank approximation. *BIT Numerical Mathematics*, pages 1–26, 2022.
- [6] G. Ceruti and C. Lubich. An unconventional robust integrator for dynamical low-rank approximation. *BIT Numerical Mathematics*, 62(1):23–44, 2022.
- [7] G. Ceruti, C. Lubich, and D. Sulz. Rank-adaptive time integration of tree tensor networks. *SIAM Journal on Numerical Analysis*, 61(1):194–222, 2023.
- [8] G. Ceruti, C. Lubich, and H. Walach. Time integration of tree tensor networks. *SIAM Journal on Numerical Analysis*, 59(1):289–313, 2021.
- [9] Y. Cheng, D. Wang, P. Zhou, and T. Zhang. Model compression and acceleration for deep neural networks: The principles, progress, and challenges. *IEEE Signal Processing Magazine*, 35(1):126–136, 2018.
- [10] Y. Cheng, F. X. Yu, R. S. Feris, S. Kumar, A. Choudhary, and S.-F. Chang. An exploration of parameter redundancy in deep networks with circulant projections. In *Proceedings of the IEEE international conference on computer vision*, pages 2857–2865, 2015.
- [11] M. Courbariaux, Y. Bengio, and J.-P. David. Training deep neural networks with low precision multiplications. In *Workshop contribution at International Conference on Learning Representations*, 2015.
- [12] M. Courbariaux, I. Hubara, D. Soudry, R. El-Yaniv, and Y. Bengio. Binarized neural networks: Training deep neural networks with weights and activations constrained to+ 1 or-1. *arXiv:1602.02830*, 2016.
- [13] L. De Lathauwer, B. De Moor, and J. Vandewalle. A multilinear singular value decomposition. *SIAM journal on Matrix Analysis and Applications*, 21(4):1253–1278, 2000.
- [14] J. Frankle and M. Carbin. The lottery ticket hypothesis: Finding sparse, trainable neural networks. In *International Conference on Learning Representations*, 2019.
- [15] M. Gabor and R. Zdunek. Compressing convolutional neural networks with hierarchical tucker-2 decomposition. *Applied Soft Computing*, 132:109856, 2023.
- [16] Y. Gong, L. Liu, M. Yang, and L. Bourdev. Compressing deep convolutional networks using vector quantization. In *International Conference on Learning Representations (ICLR)*, 2015.
- [17] Y. Guo, A. Yao, and Y. Chen. Dynamic network surgery for efficient dnns. *Advances in neural information processing systems*, 29, 2016.
- [18] S. Gupta, A. Agrawal, K. Gopalakrishnan, and P. Narayanan. Deep learning with limited numerical precision. In *International conference on machine learning*, pages 1737–1746. PMLR, 2015.
- [19] S. Han, J. Pool, J. Tran, and W. Dally. Learning both weights and connections for efficient neural network. *Advances in neural information processing systems*, 28, 2015.
- [20] Y. He, X. Zhang, and J. Sun. Channel pruning for accelerating very deep neural networks. In *Proceedings of the IEEE international conference on computer vision*, pages 1389–1397, 2017.

- [21] Y. Idelbayev and M. A. Carreira-Perpinan. Low-rank compression of neural nets: Learning the rank of each layer. In *Proceedings of the IEEE/CVF Conference on Computer Vision and Pattern Recognition (CVPR)*, June 2020.
- [22] M. Khodak, N. Tenenholz, L. Mackey, and N. Fusi. Initialization and regularization of factorized neural layers. In *International Conference on Learning Representations*, 2021.
- [23] E. Kieri, C. Lubich, and H. Walach. Discretized dynamical low-rank approximation in the presence of small singular values. *SIAM Journal on Numerical Analysis*, 54(2):1020–1038, 2016.
- [24] Y.-D. Kim, E. Park, S. Yoo, T. Choi, L. Yang, and D. Shin. Compression of deep convolutional neural networks for fast and low power mobile applications. In *International Conference on Learning Representations (ICLR)*, 2016.
- [25] O. Koch and C. Lubich. Dynamical low-rank approximation. *SIAM Journal on Matrix Analysis and Applications*, 29(2):434–454, 2007.
- [26] O. Koch and C. Lubich. Dynamical tensor approximation. *SIAM*, 31, 2010.
- [27] T. G. Kolda and B. W. Bader. Tensor decompositions and applications. *SIAM review*, 51(3):455–500, 2009.
- [28] J. Kossaifi, A. Bulat, G. Tzimiropoulos, and M. Pantic. T-net: Parametrizing fully convolutional nets with a single high-order tensor. In *Proceedings of the IEEE/CVF conference on computer vision and pattern recognition*, pages 7822–7831, 2019.
- [29] V. Lebedev, Y. Ganin, M. Rakhuba, I. Oseledets, and V. Lempitsky. Speeding-up convolutional neural networks using fine-tuned CP-decomposition. In *International Conference on Learning Representations (ICLR)*, 2015.
- [30] C. Li and C. J. R. Shi. Constrained optimization based low-rank approximation of deep neural networks. In *Proceedings of the European Conference on Computer Vision (ECCV)*, September 2018.
- [31] Y. Li, S. Gu, L. V. Gool, and R. Timofte. Learning filter basis for convolutional neural network compression. In *Proceedings of the IEEE/CVF International Conference on Computer Vision (ICCV)*, October 2019.
- [32] B. Liu, M. Wang, H. Foroosh, M. Tappen, and M. Pensky. Sparse convolutional neural networks. In *Proceedings of the IEEE Conference on Computer Vision and Pattern Recognition (CVPR)*, June 2015.
- [33] C. Lubich. Time integration in the multiconfiguration time-dependent hartree method of molecular quantum dynamics. *Applied Mathematics Research eXpress*, 2015(2):311–328, 2015.
- [34] C. Lubich and I. V. Oseledets. A projector-splitting integrator for dynamical low-rank approximation. *BIT Numerical Mathematics*, 54(1):171–188, 2014.
- [35] C. Lubich, B. Vandereycken, and H. Walach. Time integration of rank-constrained tucker tensors. *SIAM Journal on Numerical Analysis*, 56(3):1273–1290, 2018.
- [36] Z. Mariet and S. Sra. Diversity networks: Neural network compression using determinantal point processes. In *International Conference on Learning Representations (ICLR)*, 2016.
- [37] R. Mishra, H. P. Gupta, and T. Dutta. A survey on deep neural network compression: Challenges, overview, and solutions. *arXiv:2010.03954*, 2020.
- [38] P. Molchanov, S. Tyree, T. Karras, T. Aila, and J. Kautz. Pruning convolutional neural networks for resource efficient inference. In *International Conference on Learning Representations*, 2017.
- [39] M. Nagel, M. v. Baalen, T. Blankevoort, and M. Welling. Data-free quantization through weight equalization and bias correction. In *Proceedings of the IEEE/CVF International Conference on Computer Vision*, pages 1325–1334, 2019.
- [40] S. Narang, G. Diamos, S. Sengupta, and E. Elsen. Exploring sparsity in recurrent neural networks. In *International Conference on Learning Representations (ICLR)*, 2017.
- [41] A. Phan, K. Sobolev, K. Sozykin, D. Ermilov, J. Gusak, P. Tichavský, V. Glukhov, I. Oseledets, and A. Cichocki. Stable low-rank tensor decomposition for compression of convolutional neural network. In *European Conference on Computer Vision*, 2020.

- [42] S. Schotthöfer, E. Zangrando, J. Kusch, G. Ceruti, and F. Tudisco. Low-rank lottery tickets: finding efficient low-rank neural networks via matrix differential equations. In *Advances in Neural Information Processing Systems*, 2022.
- [43] D. Scieur, V. Roulet, F. Bach, and A. d’Aspremont. Integration methods and accelerated optimization algorithms. In *Advances In Neural Information Processing Systems*, 2017.
- [44] N. S. Sohoni, C. R. Aberger, M. Leszczynski, J. Zhang, and C. Ré. Low-memory neural network training: A technical report. *arXiv:1904.10631*, 2019.
- [45] D. Song, P. Zhang, and F. Li. Speeding up deep convolutional neural networks based on tucker-cp decomposition. In *Proceedings of the 2020 5th International Conference on Machine Learning Technologies*, ICMLT 2020, page 56–61, New York, NY, USA, 2020. Association for Computing Machinery.
- [46] E. Stoudenmire and D. J. Schwab. Supervised learning with tensor networks. In D. Lee, M. Sugiyama, U. Luxburg, I. Guyon, and R. Garnett, editors, *Advances in Neural Information Processing Systems*, volume 29. Curran Associates, Inc., 2016.
- [47] K. Ullrich, E. Meeds, and M. Welling. Soft weight-sharing for neural network compression. In *International Conference on Learning Representations (ICLR)*, 2017.
- [48] M. Usvyatsov, R. Ballester-Ripoll, and K. Schindler. tntorch: Tensor network learning with pytorch, 2022.
- [49] V. Vanhoucke, A. Senior, and M. Z. Mao. Improving the speed of neural networks on cpus. In *Deep Learning and Unsupervised Feature Learning Workshop, NIPS 2011*, 2011.
- [50] G. Venkatesh, E. Nurvitadhi, and D. Marr. Accelerating deep convolutional networks using low-precision and sparsity. In *2017 IEEE International Conference on Acoustics, Speech and Signal Processing (ICASSP)*, pages 2861–2865. IEEE, 2017.
- [51] H. Wang, S. Agarwal, and D. Papailiopoulos. Pufferfish: Communication-efficient models at no extra cost. *Proceedings of Machine Learning and Systems*, 3:365–386, 2021.
- [52] Z. Wang, C. Li, and X. Wang. Convolutional neural network pruning with structural redundancy reduction. In *Proceedings of the IEEE/CVF Conference on Computer Vision and Pattern Recognition*, pages 14913–14922, 2021.
- [53] G. Wanner and E. Hairer. *Solving ordinary differential equations II*, volume 375. Springer Berlin Heidelberg New York, 1996.
- [54] J. Wu, C. Leng, Y. Wang, Q. Hu, and J. Cheng. Quantized convolutional neural networks for mobile devices. In *Proceedings of the IEEE conference on computer vision and pattern recognition*, pages 4820–4828, 2016.
- [55] H. Yang, M. Tang, W. Wen, F. Yan, D. Hu, A. Li, H. Li, and Y. Chen. Learning low-rank deep neural networks via singular vector orthogonality regularization and singular value sparsification. In *Proceedings of the IEEE/CVF conference on computer vision and pattern recognition workshops*, pages 678–679, 2020.